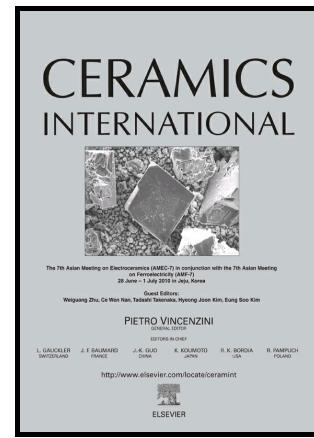# Author's Accepted Manuscript

Microwave-assisted synthesis of ZnO doped CeO$_2$ nanoparticles as potential scaffold for highly sensitive nitroaniline chemical sensor

Naushad Ahmad, Ahmad Umar, Rajesh Kumar, Manawwer Alam

CERAMICS INTERNATIONAL

The 7th Asian Meeting on Electroceramics (AMEC-7) in conjunction with the 7th Asian Meeting on Ferroelectricity (AMF-7)
28 June – 1 July 2010 in Jeju, Korea

Guest Editors:
Weiguang Zhu, Ce Wen Nan, Tadashi Takenaka, Hyeong Joon Kim, Eung Soo Kim

PIETRO VINCENZINI
GENERAL EDITOR

EDITORS-IN-CHIEF

| L. GAUCKLER SWITZERLAND | J. F. BAUMARD FRANCE | J.-K. GUO CHINA | K. KOUMOTO JAPAN | R. K. BORDIA USA | R. PAMPUCH POLAND |

http://www.elsevier.com/locate/ceramint

ELSEVIER

www.elsevier.com/locate/ceri

Cite this article as: Naushad Ahmad, Ahmad Umar, Rajesh Kumar and Manawwer Alam, Microwave-assisted synthesis of ZnO doped CeO nanoparticles as potential scaffold for highly sensitive nitroaniline chemica sensor, *Ceramics International*, http://dx.doi.org/10.1016/j.ceramint.2016.04.01:

This is a PDF file of an unedited manuscript that has been accepted fo publication. As a service to our customers we are providing this early version o the manuscript. The manuscript will undergo copyediting, typesetting, and review of the resulting galley proof before it is published in its final citable form. Please note that during the production process errors may be discovered which could affect the content, and all legal disclaimers that apply to the journal pertain

Microwave-assisted synthesis of ZnO doped CeO₂ nanoparticles as potential scaffold for highly sensitive nitroaniline chemical sensor

Naushad Ahmad[1], Ahmad Umar[2,3]*Rajesh Kumar,[4]Manawwer Alam[5]

[1]Department of Chemistry, College of Science, Riyadh-11451, King Saud University, Kingdom of Saudi Arabia

[2]Promising Centre for Sensors and Electronic Devices (PCSED), Najran University, P.O.Box-1988, Najran-11001, Kingdom of Saudi Arabia

[3]Department of Chemistry, College of Science and Arts, Najran University, P.O.Box-1988, Najran-11001, Kingdom of Saudi Arabia

[4]PG Department of Chemistry, JCDAV College (Panjab University) Dasuya-144205, Punjab, India

[5]Research Centre, College of Science, Riyadh-11451, King Saud University, Kingdom of Saudi Arabia

*Corresponding author:

Email: ahmadumaresn@gmail.com

Abstract

Herein, we report the successful fabrication of highly sensitive, reproducible and reliable nitroaniline chemical sensor based on ZnO doped CeO₂ nanoparticles. The ZnO doped CeO₂ nanoparticles were synthesized through a simple, facile and rapid microwave-assisted method and characterized by several techniques. The detailed characterizations confirmed that the synthesized nanoparticles are monodisperse and grown in high density and possessing good crystallinity. Further, the synthesized ZnO doped CeO₂nanoparticles were used as efficient electron mediators for the fabrication of high sensitive nitroaniline chemical sensors. The

fabricated nitroaniline chemical sensor exhibited very high sensitivity of $550.42\mu A.mM^{-1}cm^{-2}$ and experimental detection limit of 0.25 mM. To the best of our knowledge, this is the first report in which CeO_2-ZnO nanoparticles were used as efficient electron mediators for the fabrication of nitroaniline chemical sensors. Thus, presented work demonstrates that ZnO doped CeO_2 nanoparticles are potential material to fabricate highly efficient and reliable chemical sensors.

Keywords: ZnO doped CeO_2; nanoparticles, Chemical sensors; Nitroaniline

1. Introduction

Recently, doped and composite lanthanide oxide materials have been explored extensively for a variety of applications. Ceria (CeO_2) is one of the most studied oxide among the various lanthanide oxides owing to its excellent mechanical strength, high oxygen storage capacity (OSC), good optical properties, high conductivity, good redox performances, high specific surface area particularly in nano regime, high thermal stability, abundance of active sites and oxygen vacancies on the surface, and most importantly low cost synthesis [1, 2]. These properties make this material a promising candidate for a number of applications. The performance of these properties, and hence the versatility for potential applications can be enhanced by either doping or making its composites with other metals or metal oxides. Transition metal like Ni, Cu, Zn, Co, Sc, Y, Zr, Ti , Fe [3-10]and metal oxides such as ZnO, TiO_2, CuO, CaO, NiO, Tb_2O_3, MnO_2[11-21]*etc*. are some of the reported examples of dopants and additive materials, respectively for CeO_2. Doped or composite CeO_2 materials are potentially

used as photocatalysts **[22-24]**, electrochemical sensors **[25, 26],** gas sensors**[27, 28]**, biosensors**[29, 30]**, anodic materials for fuel cells and lithium ion batteries**[31]**, super-capacitors**[19]**, catalyst for CO oxidation**[16, 32]**,electrochemical charge storage devices **[33, 34]** and many more. Singh et al.**[25]**successfully synthesized well crystalline CeO_2-ZnO nano-ellipsoids via facile hydrothermal process at low-temperature conditions. These nano-ellipsoids exhibited a high sensitivity of ~0.120 $\mu A/\mu Mcm^2$ with a low detection limit of 1.163 μM for p-nitrophenol.

CeO_2-ZnO hexagonal nanodisks synthesized via chemical route at low-temperature by Lamba et al. **[22]**. The prepared hexagonal nanodisks were acted as an efficient photocatalyst for the degradation of Direct Blue-15 dye under solar light irradiation. Hamedani et al. **[27]** reported that ZnO nanostructures doped with 5 wt% CeO_2 showed improved gas sensing response, reduced recovery time and highly selective sensing of ethanol even in the presence of CO and CH_4. It was proposed that large oxygen storage capacity and the presence of a large number of oxygen vacancies on the surface of CeO_2 with fluorite structure deposited over ZnO surface resulted in the rapid diffusion of oxygen, easily oxidizing the analyte molecules**[35, 36]**. Similar results were observed by Rajgure et al. **[28]**for 2 wt% CeO_2 doped ZnO nanocomposites. He et al. fabricated dumbbell-like ZnO nanoparticles deposited over the surface of CeO_2 nanorods via the hydrothermal method and reported excellent electrochemical performance as compared to pure CeO_2 nanorods. Li et al **[37]** and Wan et al. **[38]** observed high sensitivity and selectivity with fast response for sensors based on Ce-doped ZnO hollow nanofibers, synthesized through facile single capillary electro-spinning technique, as compared to pure ZnO nanomaterials. Similarly, Yan et al. **[39]** reported ethanol sensing applications of porous CeO_2–ZnO hollow fibers synthesized on cotton bio-template.

Doping is supposed to influence the active surface area, surface defects, oxygen vacancies and the diffusion rates. Due to the presence of surface defects and oxygen vacancies, cerium can undergo fast and reversible Ce^{+4}-Ce^{+3} redox interconversions [27]. Both CeO_2 (Eg=3.15eV) and ZnO (Eg=3.37) are n-type semiconductors and thus form n–n type hetero-junction [1, 12, 39]. The electronic transitions in such heterojunctions result in the formation of an electron depletion layer at the interface of ZnO and CeO_2, thereby improving the electrocatalytic properties [40]. Thus, CeO_2–ZnO materials can efficiently act as transducers for converting chemical energies produced during redox processes occurring at their surface into electrical signals.

In this paper, well crystalline ZnO doped CeO_2composite nanoparticles were synthesized by the facile chemical microwave-assisted process. The prepared nanoparticles were characterized in detail using different characterization techniques. Further, the synthesized nanoparticles were used as potential electron mediators for the fabrication of nitroaniline chemical sensors. To the best of our knowledge, this is the first report in which well-crystalline ZnO doped CeO_2 composite nanoparticles were used as efficient electron mediator to fabricate highly sensitive nitroaniline chemical sensor.

2. Experimental details

2.1. Materials

All chemicals procured for the synthesis ZnO doped CeO_2 nanoparticles were used as received without any further purifications. For the synthesis, Zinc Chloride and Cerium Nitrate were obtained from BDH Chemicals Ltd Poole England, Ammonia Solution (about35%) was procured from Avonchem, Cheshire, UK.

2.2. Synthesis of ZnO doped CeO$_2$ nanoparticles

In order to synthesize ZnO doped CeO$_2$ nanoparticles, 50 mL of 0.25M Zinc chloride solution was mixed with 50 mL equimolar solution of cerium nitrate with continuous stirring. The pH of the reaction solution was adjusted to 8 by the careful dropwise addition of 1:1 aqueous NH$_3$ solution. All the solutions were made in triple de-ionized (DI) water. The reaction solution was then transferred to a Teflon microwave beaker and the contents were subjected to microwave treatment for 30 min at 200°C temperature in a Microwave oven (MicroSynth Plus Model, Milestone, US). After the completion of the reaction, the solution was allowed to cool to room temperature followed by the filtration and washings with distilled water for several times to remove any unreacted compound. The yellowish white product was dried in an air oven for 6h at 70°C.

2.3. Characterizations of ZnO doped CeO$_2$ nanoparticles

The detailed analysis for the structural, morphological, microstructural and compositional of ZnO doped CeO$_2$ composites nanoparticles was carried out using different techniques. Field emission scanning electron microscopy (FESEM; JEOL-JSM-7600F) and high-resolution TEM (HR-TEM) were used for morphological and structural analysis. The phases, micro-structural properties and crystallinity of ZnO doped CeO$_2$ composites nanoparticles was studied by X-ray diffraction (XRD; PAN analytical Xpert Pro.) in the scan range of 15-75° (2θ) using Cu-Kα radiation (λ=1.54178Å). Fourier transform infrared spectroscopic analysis (FTIR; Perkin Elmer-FTIR Spectrum-100) was used for the compositional studies of the composites with KBr pelletization in the scan range of 450-4000 cm^{-1}. For FTIR characterization, the ZnO doped CeO$_2$

powder was mixed with dry solid KBr and ground to a fine powder with the help of mortar and pestle. Finally, the ground powder was pressed to form a transparent pellet. The scattering property of ZnO doped CeO_2 composite nanoparticles was studied at room temperature by using Raman-scattering spectroscopy in the scan range of 200-800 cm^{-1}(Perkin Elmer-Raman Station 400 series).

2.4. Fabrication of nitroaniline chemical sensor based on ZnO doped CeO₂ nanoparticles

For the fabrication of electrochemical sensor, ZnO doped CeO_2nanoparticles were mixed with conducting agent butyl carbital acetate (BCA) to form a homogeneous and thin paste which was pasted on the surface of pre-cleaned silver (Ag) electrode. To fix the sensor material layer on the surface of the Ag electrode, it was dried in an air oven for 6h at 70-72°C. For measuring the electrochemical sensing parameters Keithley 6517A, USA electrometer was used as a source of voltage and to record the current. ZnO doped CeO_2nanoparticlesmodified Ag electrode (AgE) and Pt wire was used as working and counter electrodes, respectively. All the experiments were performed at room temperature in the presence of 0.1M phosphate buffer solution (PBS) with pH=7.4.

3. Results and discussion

3.1. Characterizations and properties of ZnO doped CeO₂ nanoparticles

The morphological properties of the ZnO doped CeO_2nanoparticles were characterized by field emission scanning electron microscopy (FESEM) and transmission electron microscopy (TEM).

Figure 1 (a) exhibits the typical low-magnification FESEM image of synthesized ZnO-doped CeO_2 which confirmed that the prepared materials are nano-sized particles which are

grown in very high density. The nanoparticles are monodisperse and spherical in shape. Most of the nanoparticles possess similar sizes while some small nanoparticles are also seen in the micrograph (figure 1(b)). Figure 1 (c) and (d) depict the typical TEM images of synthesized ZnO doped CeO_2 nanoparticles which revealed that the nanoparticles are grown in high density. As it can be seen from the observed TEM images that due to high-density growth some agglomeration in the nanoparticles is also seen. The prepared ZnO doped CeO_2 nanoparticles possess different sizes with almost spherical shapes and are well dispersed.
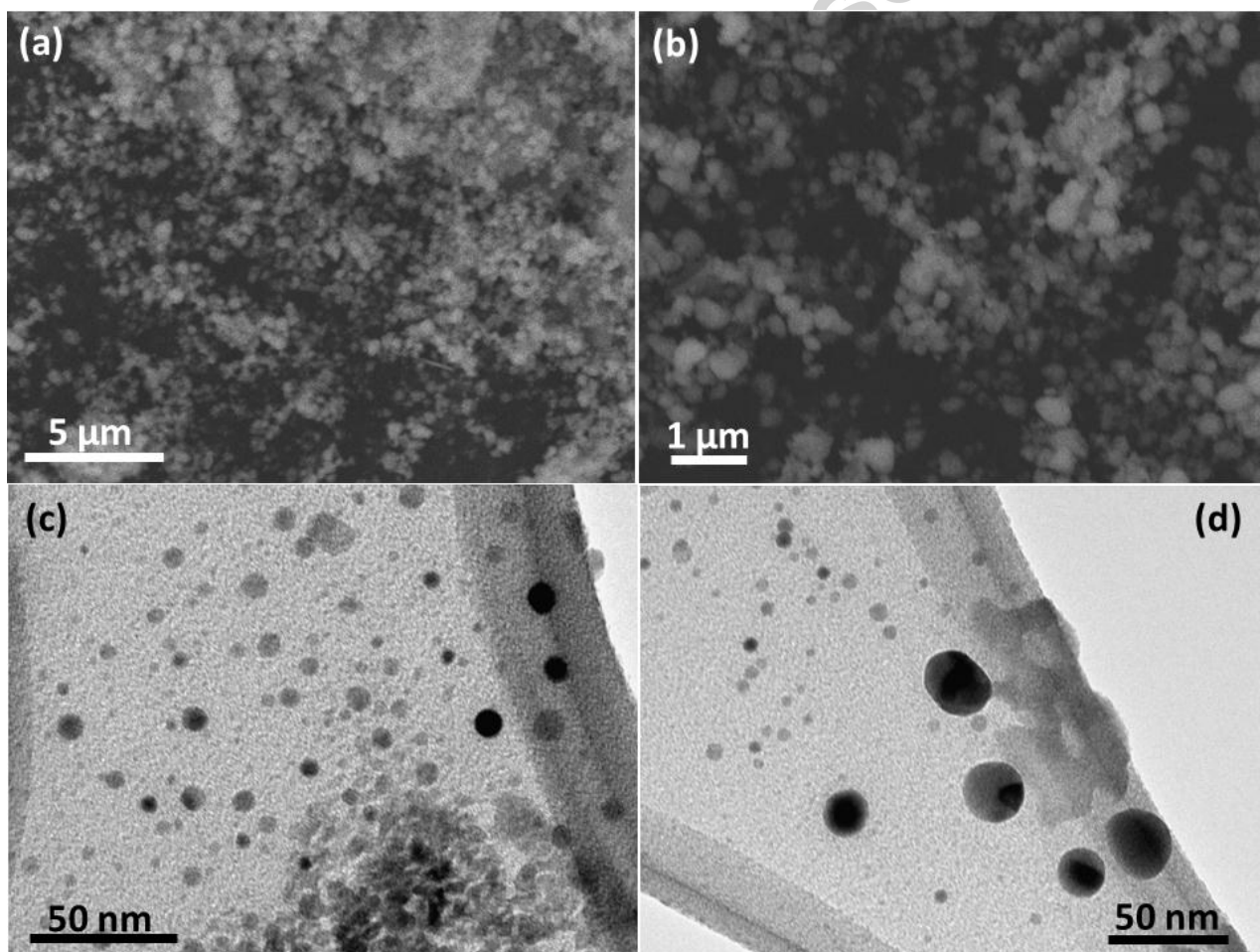
Fig.1.(a) Low and **(b)** high-resolution FESEM images and **(c and d)** TEM images of ZnO doped CeO$_2$ nanoparticles.

Figure 2 represents the XRD patterns of the ZnO doped CeO$_2$nanoparticles. Well defined diffraction peaks at diffraction angles at 2θ = 28.6^o, 33.05^o, 47.64^o, 56.49^o, 59.16^o, and 69.72^{o}corresponds to the (111), (200), (220), (311), (222) and (400) planes of cubic ceria (CeO$_2$) phase with fluorite structure, respectively (JCPDS card number 34-394) **[1, 22, 25, 41]**. On the other hand, the diffraction patterns at 2θ = 36.33^o, 62.93^o and 68.03^{o}are the characteristics peaks corresponding to (101), (103) and (112) diffraction planes of wurtzite hexagonal phase of ZnO (JCPDS card no. 36-1451) **[42-44]**.No other diffraction peak in the XRD spectrum except for CeO$_2$ and ZnO confirms the fact that composites are of high purity and are composed of onlyCeO$_2$ and ZnO. Well-defined and sharp reflections of the XRD peaks reveal the good crystallinity of the ZnO doped CeO$_2$nanoparticles. The obtained XRD patterns also match well with the reported literature.
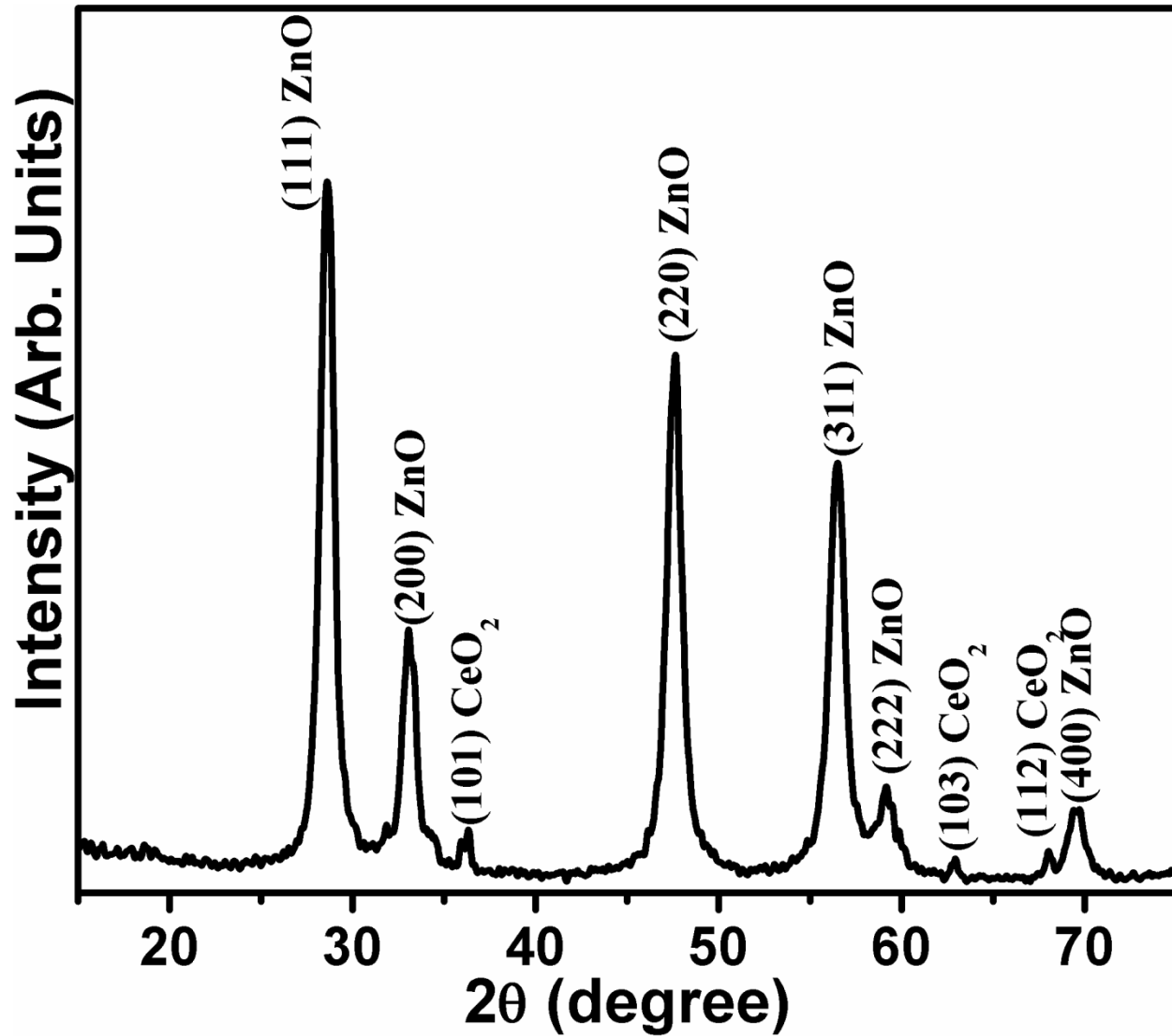
Fig.2. Typical XRD diffraction patterns of ZnO doped CeO$_2$ nanoparticles.

The crystallite sizes of ZnO and CeO$_2$ were determined from Debye–Scherrer formula (Eq.1).

$$d = \frac{0.89\lambda}{\beta.Cos\theta} \ldots\ldots\ldots(1)$$

Where λ= the wavelength of X-rays used (0.1541 nm), θ is the Bragg diffraction angle corresponding to ZnO (101) peak situated at $36.33^{\circ}$and CeO_2 (111) peak at $28.60^{\circ}$and β is the peak width at half maximum (FWHM) **[36, 45]**. The values for β, as derived from the XRD patterns were 0.32873 and 0.92124 for ZnO and CeO_2, respectively. The crystallite sizes of the ZnO nanoparticles and CeO_2were found to be 25.17 and 8.81 nm, respectively.

To study the chemical composition of the ZnO doped CeO_2nanoparticles, FTIR studies were performed and the results are represented in Figure 3.Three well-defined absorption peaks at 470.63, 1633.71 and 3456.44 cm^{-1}were observed. Sharp and strong absorption peak at 470.63 $cm^{-1}$is related to the M–O mode (Ce−O and Zn−O)**[11-13]**.Other two well-defined absorption peaks at 1633.71$cm^{-1}$and 3456.44 cm^{-1} may be assigned to the bending vibrational modes of the absorbed H_2O and surface O−H stretching modes, respectively**[27, 28]**. No other absorption peaks except for the above-mentioned peaks in the FTIR spectrum further confirms the purity of synthesized ZnO doped CeO_2nanoparticles.
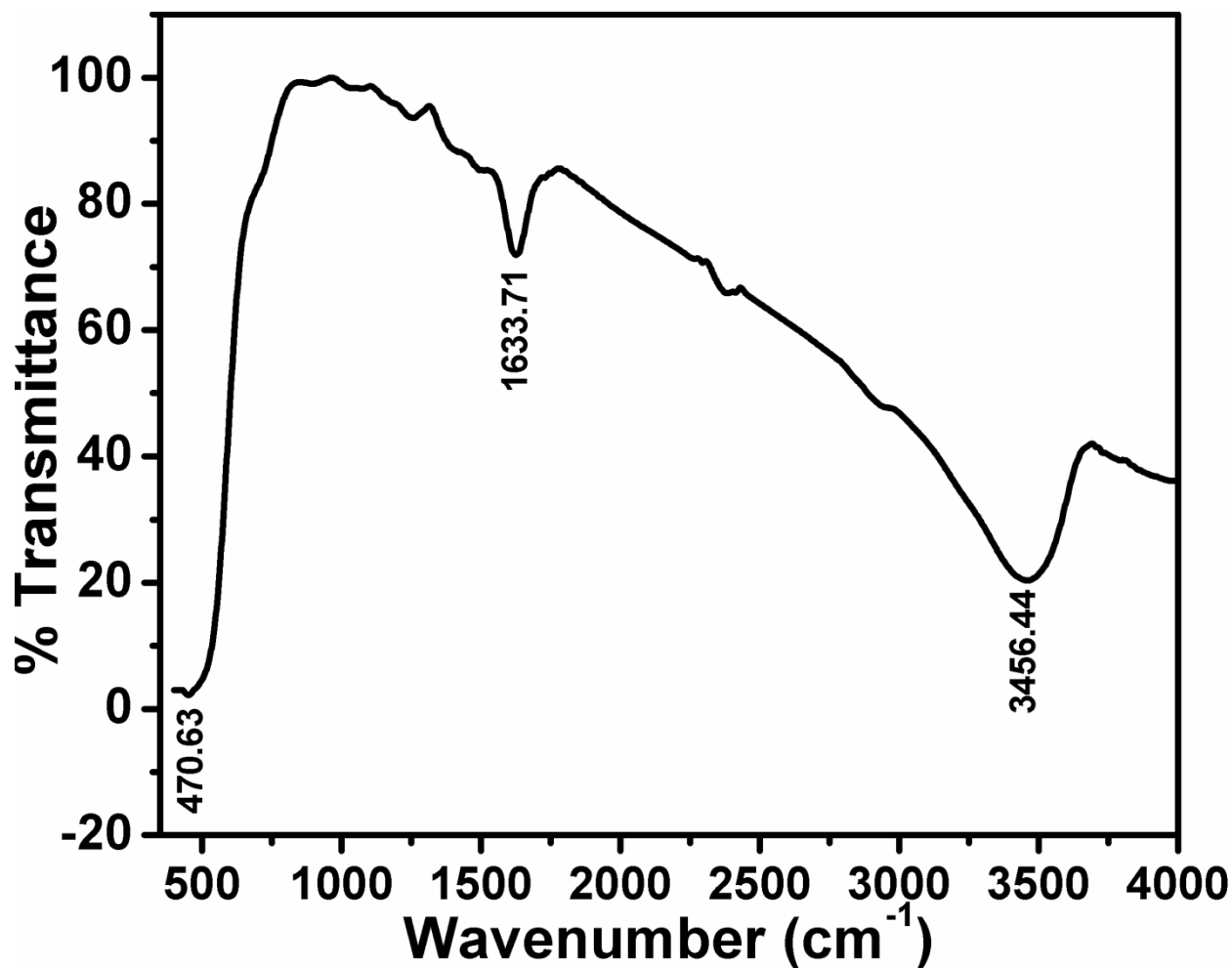
Fig.3. Typical FTIR spectrum of ZnO doped CeO₂ nanoparticles.

The Raman scattering spectrum of the ZnO doped CeO₂nanoparticles is represented in Figure 4. In order to study scattering properties of prepared CeO2-ZnO NEs were investigated by Raman scattering spectrum and observed result is demonstrated in figure 3 (b). Two sharp and well-defined peaks at 462 cm^{-1}and 436 cm^{-1}can be clearly seen. The sharp intense peak at 462 cm^{-1}is the characteristic peak for the fluorite cubic structure of CeO$_2$ and is assigned to F$_{2g}$ mode, whereas the low-intensity peak at 436 cm^{-1} is assigned to E_2^{High} mode of wurtzite hexagonal structure of ZnO corresponding to non-polar optical phonons [26, 29, 34] .The peaks in Raman scattering spectrum are also well matched with the reported literature [46, 47].
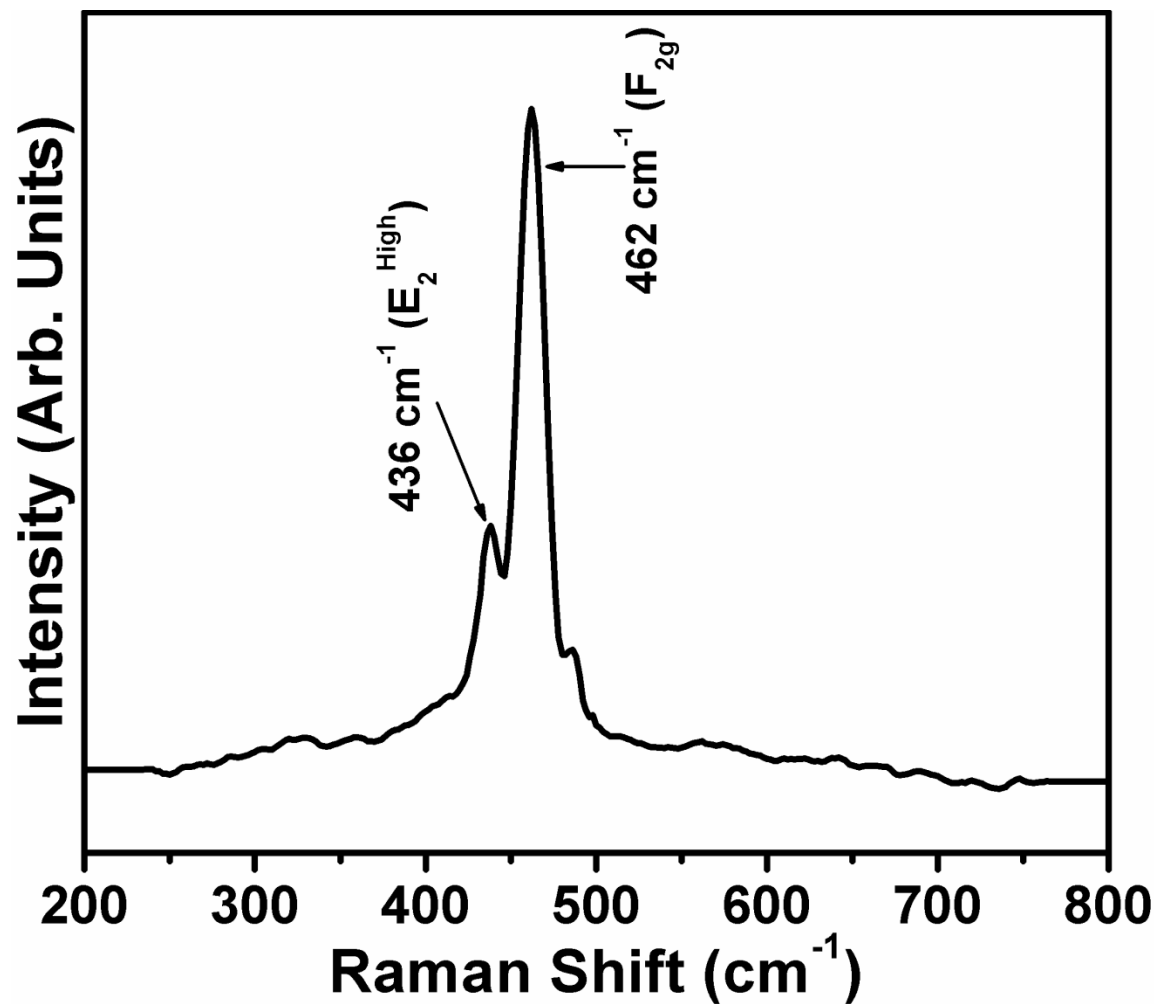
Fig. 4. Typical Raman-scattering spectrum of ZnO doped CeO$_2$ nanoparticles.

3.2. Nitroaniline chemical sensing applications of ZnO doped CeO$_2$ nanoparticles

Current –voltage technique was employed for the measurements of the electric responses of the ZnO doped CeO$_2$ nanoparticlestoward nitroaniline in PBS with physiological pH of 7.4. Figure5 shows a remarkable increase in the current (μA) for PBS containing even very low concentration (0.25 mM) of nitroaniline. At a potential of 1.5 V, the high electric response of 26.84 μA was recorded for nitroaniline solution as compared to very low 7.56 μA response for

blank PBS. Hence, ZnO doped CeO₂nanoparticlescan efficiently act as excellent electron mediators for the sensing and detection of very low concentrations of nitroaniline.
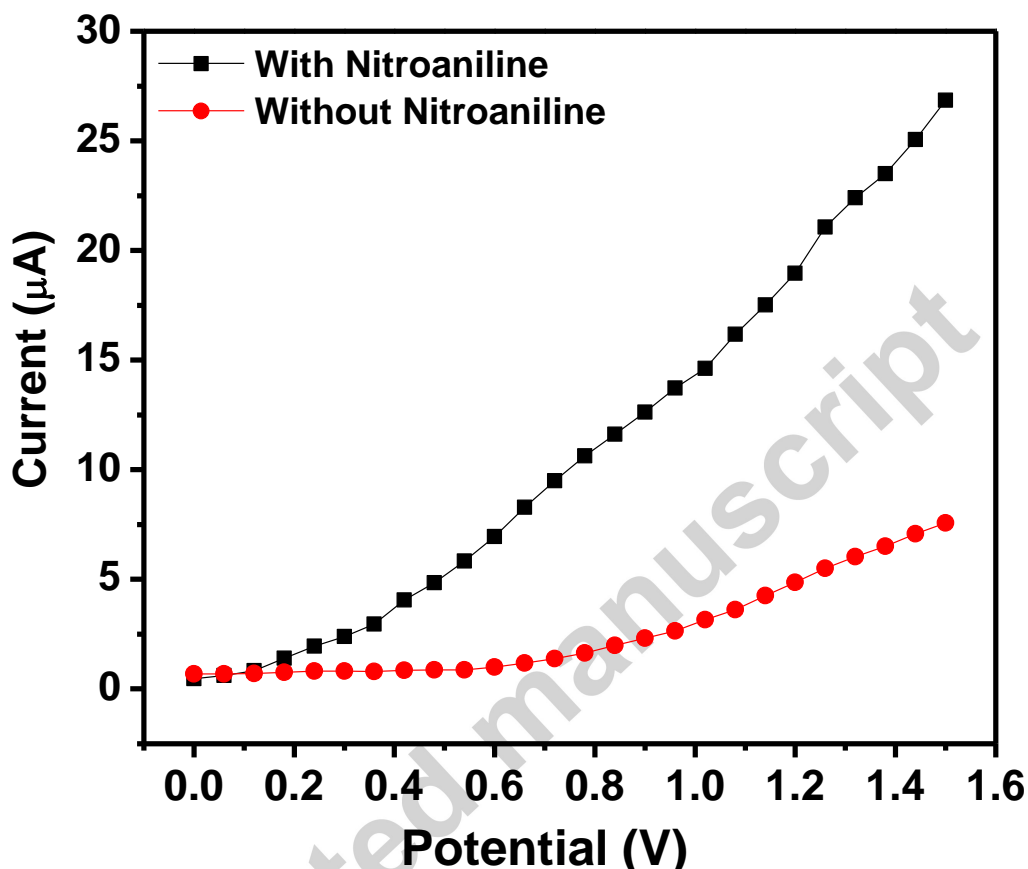

Fig.5. The current-voltage performances of modified silver electrode (AgE) with ZnO doped CeO2 nanoparticles in PBS solution with 0.25 mM nitroaniline and without nitroaniline.

A strong positive correlation between the current magnitude and concentration of the nitroaniline is shown in Figure 6 (a). When nitroaniline solutions with concentrations 0.25, 0.50, 1.0, 2.0, 3.0, 4.0 and 5.0 mM were subjected to current –voltage analysis using ZnO doped CeO₂nanoparticlesmodified AgE, current magnitudes of 26.84, 37.81, 46.77, 55.87, 64.29, 74.73 and 89.96µA were recorded at 1.5 V potential in PBS at room temperature. In order to check the reproducibility of the ZnO doped CeO₂ nanoparticles toward electrochemical sensing of nitroaniline, experiments were repeated for three consecutive weeks without and further

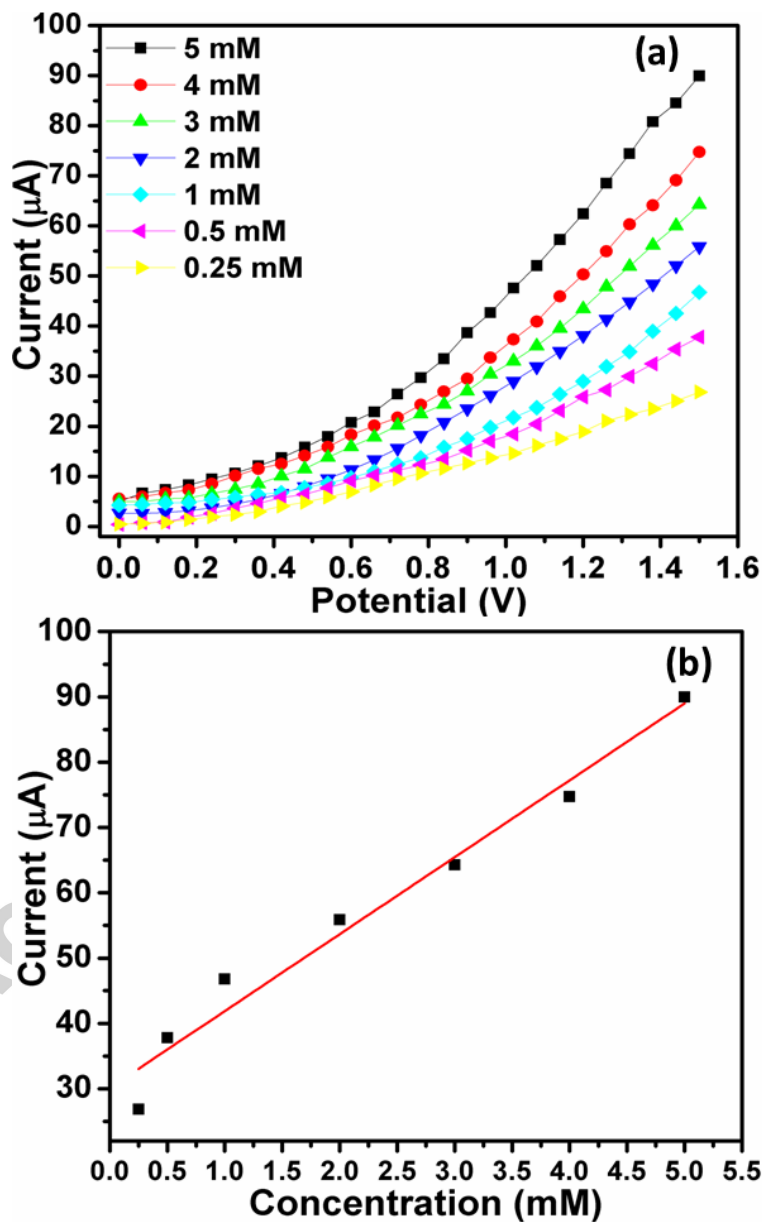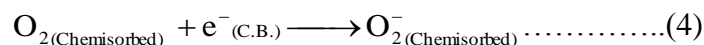modification of the sensors. All the observed results were in good agreement with the previous results.
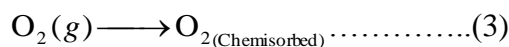

Fig.6.(a) Current-Voltage responses for various concentrations of nitroaniline and **(b)** Calibration curve for nitroaniline using ZnO doped CeO_2 nanoparticles modified AgE.
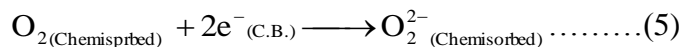
The parameters like sensitivity, linear dynamic range (LDR) and limit of detection (LOD) for the ZnO doped CeO$_2$ nanoparticles modified AgE sensors were estimated for the calibration curve plotted between concentrations of the nitroaniline and the current responses. The corresponding graph is represented in Figure 6 (b).Sensitivity is defined as the ratio of the slope of the calibration curve to the active surface area of the working AgE (Eq.-2) **[48-50]**. The high sensitivity of 550.42μA.mM^{-1}cm^{-2} and experimental low detection limit of 0.25 mM were estimated from the observed calibration plot. The LDR for ZnO doped CeO$_2$ nanoparticles modified AgE sensor range from 0.25 mM –5.0 mM with a correlation coefficient (R) of 0.98597.

$$\text{Sensitivity} = \frac{\text{Slope of the calibration curve}}{\text{Active surface area of the working AgE}} \ldots\ldots\ldots\ldots(2)$$

3.3. Sensing mechanism

As reported in the literature, the chemisorbed oxygen (O$_2$) molecules on the surface of nanomaterials either from the reaction medium or from the surrounding environment play a crucial role in the detection and sensing of analyte species **[51-53]**. Additionally, ZnO doping increases the porosity as well as the surface area of the CeO$_2$ sheets for a greater extent of adsorption. The O$_2$ molecules on the surface of the ZnO doped CeO$_2$ are converted to oxygenated anionic species such as superoxides (O_2^-), peroxides (O_2^{2-}) and even oxides (O^{2-}) through capturing conduction band electrons of the sensor material coated on the surface of Ag electrode **[53, 54]** (Eq.3-5).

$$\text{O}_2(g) \longrightarrow \text{O}_{2(\text{Chemisorbed})} \ldots\ldots\ldots\ldots..(3)$$

$$\text{O}_{2(\text{Chemisorbed})} + \text{e}^-_{(\text{C.B.})} \longrightarrow \text{O}^-_{2(\text{Chemisorbed})} \ldots\ldots\ldots\ldots..(4)$$

$$O_{2\,(Chemisprbed)} + 2e^-{}_{(C.B.)} \longrightarrow O_2^{2-}{}_{(Chemisorbed)} \cdots\cdots(5)$$

The resistance of the ZnO doped CeO$_2$nanoparticlesa sensor material is thus increased in the absence of nitroaniline. In contrast, when nitroaniline is added to the solution, the chemisorbed species on the surface of the ZnO doped CeO$_2$nanoparticlesbased sensors; reduce the –NO$_2$ group of the nitroaniline to hydroxylamine group initially followed by reversible oxidation to less toxic nitroso group. The release of the electrons to the conduction band during the oxidation process increases the conductivity and hence the current magnitude in the presence of the nitroaniline. These redox changes catalyzed through ZnO doped CeO$_2$nanoparticlessensors are responsible for the sensing behavior of as-synthesized materials. The proposed schematic sensing mechanism is shown in Figure 7.
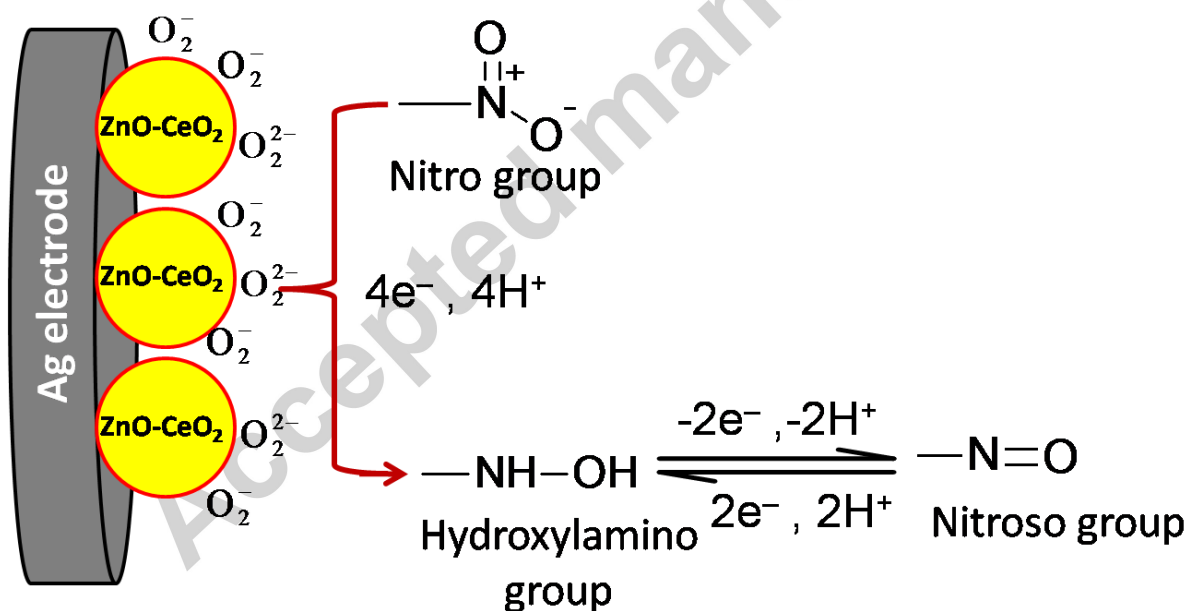

Fig.7. A proposed sensing mechanism for the ZnO doped CeO$_2$ nanoparticles modified AgE toward nitroaniline sensing.

4. Conclusion

In summary, ZnO doped CeO_2 nanoparticles were successfully synthesized by facile and simple microwave assisted process and characterized in detail in terms of their morphological, structural, compositional and scattering properties. The detailed characterizations confirmed that the nanoparticles were grown in high-density and possessing well-crystalline structures. Interestingly, the prepared ZnO doped CeO_2 nanoparticles were used as an excellent electron mediators to fabricate nitroaniline chemical sensor. The fabricated nitroaniline chemical sensor exhibited very high and reproducible sensitivity of $550.42\mu A.mM^{-1}cm^{-2}$ and experimental detection limit of 0.25 mM. Importantly, to the best of our knowledge, this is the first ever report which demonstrates the utilization of CeO_2-ZnO nanoparticles for the fabrication of highly sensitive and reproducible nitroaniline chemical sensors.

Acknowledgement

References

1. A. Umar, R. Kumar, M.S. Akhtar, G. Kumar, S.H. Kim, Growth and properties of well-crystalline cerium oxide (CeO_2) nanoflakes for environmental and sensor applications, J. Colloid Interface Sci.454 (2015) 61-68.

2. X. Du, D. Jiang, S. Chen, L. Dai, L. Zhou, N. Hao, T. You, H. Mao, K. Wang, CeO_2 nanocrystallines ensemble-on-nitrogen-doped graphene nanocomposites: one-pot, rapid

synthesis and excellent electrocatalytic activity for enzymatic biosensing, Biosens. Bioelectron. http://dx.doi.org/10.1016/j.bios.2015.11.054

3. S. Kumar, Y.J. Kim, B.H. Koo, C.G. Lee, Structural and magnetic properties of Ni doped CeO_2 nanoparticles, J. Nanosci. Nanotechnol. 10(11) (2010) 7204-7207.

4. A. Thurber, K.M. Reddy, V. Shutthanandan, M.H. Engelhard, C. Wang, J. Hays, A. Punnoose, Ferromagnetism in chemically synthesized CeO_2 nanoparticles by Ni doping. Phys. Rev. B 76 (16) (2007) 165206.

5. A.B. Kehoe, D.O. Scanlon, G.W. Watson, Role of lattice distortions in the oxygen storage capacity of divalently doped CeO_2, Chem. Mater. 23(20) (2011) 4464-4468.

6. L.R. Shah, B. Ali, H. Zhu, W.G. Wang, Y.Q. Song, H.W. Zhang, S.I. Shah, J.Q. Xiao, Detailed study on the role of oxygen vacancies in structural, magnetic and transport behavior of magnetic insulator: $Co–CeO_2$, J. Phys.: Condens. Matter. 21(48) (2009) 486004.

7. N.I. Santha, M.T. Sebastian, P. Mohanan, N.M. Alford, K. Sarma, R.C. Pullar, S. Kamba, A. Pashkin, P. Samukhina, J. Petzelt, Effect of Doping on the Dielectric Properties of Cerium Oxide in the Microwave and Far-Infrared Frequency Range, J. Am. Ceram. Soc. 87(7) (2004)1233-1237.

8. Q.Y. Wen, H.W. Zhang, Y.Q. Song, Q.H. Yang, H. Zhu, J.Q. Xiao, Room-temperature ferromagnetism in pure and Co doped CeO_2 powders,J. Phys.: Condens. Matter. 19(24) (2007) 246205.

9. Z. Tianshu, P. Hing, H. Huang, J. Kilner, Early-stage sintering mechanisms of Fe-doped CeO_2, J. Mater. Sci. 37(5) (2002) 997-1003.

10. T. Tabakova, V. Idakiev, J. Papavasiliou, G. Avgouropoulos, T. Ioannides, Effect of additives on the WGS activity of combustion synthesized CuO/CeO_2 catalysts, Catal. Commun. 8(1) (2007)101-106.

11. Ahmad Umar, A. Al-Hajry, R. Ahmad, S. Ansari, M. S. Al-Assiri, H. Algarni, Fabrication and characterization of a highly sensitive hydroquinone chemical sensor based on iron-doped ZnO nanorods, Dalton Transactions 44 (2015) 21081-21087

12. M. Shaheer Akhtar, A facile synthesis of ZnO nanoparticles and its application as photoanode for dye sensitized solar cells, Sci. Adv. Mater. 7 (2015) 1137-1142.

13. R. Li, S. Yabe, M. Yamashita, S. Momose, S. Yoshida, S. Yin, T. Sato, Synthesis and UV-shielding properties of ZnO-and CaO-doped CeO_2 via soft solution chemical process, Solid State Ionics151(1) (2002) 235-241.

14. B.M. Reddy, A. Khan, P. Lakshmanan, M. Aouine, S. Loridant, J.C. Volta, Structural characterization of nanosized CeO_2-SiO_2, CeO_2-TiO_2, and CeO2-ZrO_2 catalysts by XRD, Raman, and HREM techniques, J. Phys. Chem. B 109(8) (2005) 3355-3363.

15. C. Tsonos, A. Kanapitsas, G. C. Psarras, T. Speliotis, Effect of ZnO nanoparticles on the dielectric/electrical and thermal properties of epoxy-based nanocomposites, Sci. Adv. Mater. 7 (2015) 588-597.

16. C.A. Chagas, E.F. de Souza, R.L. Manfro, S.M. Landi, M.M. Souza, M. Schmal, Copper as promoter of the NiO–CeO_2 catalyst in the preferential CO oxidation, Appl. Catal., B: Environmental 182 (2016) 257-265.

17. J.O. Jun, J. Lee, K. H. Kang, I. K. Song, Synthesis of dimethyl carbonate from ethylene carbonate and methanol over nano-catalysts supported on CeO_2-MgO, J. Nanosci. Nanotechnol. 15 (2015) 8330-8335.

18. N.S. Arul, D. Mangalaraj, T.W. Kim, Photocatalytic degradation mechanisms of CeO_2/Tb_2O_3 nanotubes, Appl. Surf. Sci. 349 (2015) 459-464.

19. H. Zhang, J. Gu, J. Tong, Y. Hu, B. Guan, B. Hu, J. Zhao, C. Wang, Hierarchical porous MnO_2/CeO_2 with high performance for supercapacitor electrodes, Chem. Eng. J.286 (2016) 139-149.

20. L. Yu, X. Yu, T. Sun, N. Wang, Preparation for CeO_2/nanographite composite materials and electrochemical degradation of phenol by CeO_2/nanographite cathodes, J. Nanosci. Nanotechnol. 15 (2015) 4920-4925.

21. X. Chen, Q. Gao, D. Xiang, H. Lin, X. Han, X. Li, S. Du, F. Qu, Controllable fabrication of porous ZnOanofibers by electrospun with enhanced acetone sensing property, Sci. Adv. Mater. 7 (2015) 526-531.

22. R. Lamba, A. Umar, S.K. Mehta, S.K. Kansal, CeO_2-ZnO hexagonal nanodisks: Efficient material for the degradation of direct blue 15 dye and its simulated dye bath effluent under solar light,J. Alloys Compd. 620 (2015) 67-73.

23. G.S. Josephine, S. Ramachandran, A. Sivasamy, Nanocrystalline ZnO doped lanthanide oxide: An efficient photocatalyst for the degradation of malachite green dye under visible light irradiation, Journal of Saudi Chemical Society 19(5) (2015) 549-556.

24. D. Channei, B. Inceesungvorn, N. Wetchakun, and S. Phanichphant, Synthesis of $Fe_3O_4/SiO_2/CeO_2$ core-shell magnetic and their application as photocatalyst, J. Nanosci. Nanotechnol. 14 (2014) 7756-7762.

25. K. Singh, A.A. Ibrahim, A. Umar, A. Kumar, G.R Chaudhary, S. Singh, S.K. Mehta, Synthesis of CeO_2–ZnO nanoellipsoids as potential scaffold for the efficient detection of 4-nitrophenol, Sens. Actuators, B: Chemical 202 (2014) 1044-1050.

26. A. Mujtaba, N.K. Janjua, Electrochemical sensing platform based on CuO@CeO$_2$ hybrid oxides,J. Electroanal. Chem. 763 (2016) 125-133.

27. N.F. Hamedani, A.R. Mahjoub, Y. Mortazavi, CeO$_2$ doped ZnO flower-like nanostructure sensor selective to ethanol in presence of CO and CH$_4$, Sens. Actuators, B: Chemical169 (2012) 67-73.

28. A.V. Rajgure, N.L. Tarwal, J.Y. Patil, L.P. Chikhale, R.C. Pawar, C.S. Lee, I.S. Mulla, S.S. Suryavanshi, Gas sensing performance of hydrothermally grown CeO$_2$–ZnO composites, Ceram. Int. 40(4) (2014) 5837-5842.

29. D. Patil, N.Q. Dung, H. Jung, S.Y. Ahn, D.M. Jang, D. Kim, Enzymatic glucose biosensor based on CeO$_2$ nanorods synthesized by non-isothermal precipitation, Biosens. Bioelectron. 31(1) (2012) 176-181.

30. Y. Temerk, H. Ibrahim, A new sensor based on In doped CeO$_2$ nanoparticles modified glassy carbon paste electrode for sensitive determination of uric acid in biological fluids,Sens. Actuators, B: Chemical 224 (2016) 868-877.

31. T.H. Shin, S. Ida, T. Ishihara, Doped CeO$_2$–LaFeO$_3$ composite oxide as an active anode for direct hydrocarbon-type solid oxide fuel cells, J. Am. Chem. Soc. 133(48) (2011) 19399-19407.

32. Z.Y. Pu, X.S. Liu, A.P. Jia, Y.L. Xie, J.Q. LuM.F. Luo, Enhanced activity for CO oxidation over Pr-and Cu-doped CeO$_2$ catalysts: effect of oxygen vacancies,J. Phys. Chem. C112(38) (2008) 15045-15051.

33. W. Y. Jung, K.-T. Lim, S.-S. Hong, Catalytic combustion of benzene over CuO-CeO$_2$ mixed oxides, J. Nanosci. Nanotechnol. 14 (2014) 8507-8511.

34. G. He, H. Fan, L. Ma, K. Wang, C. Liu, D. Ding, L. Chen, Dumbbell-like ZnO nanoparticles-CeO_2 nanorods composite by one-pot hydrothermal route and their electrochemical charge storage, Appl. Surf. Sci. 366 (2016) 129–138.

35. F. Meng, L. Wang, J. Cui, A. Li, H. Tang, Experimental and theoretical investigations of the origin of magnetism in undoped CeO_2, Sci. Adv. Mater. 7 (2015) 663-669.

36. R.K. Hailstone, A.G. Di Francesco, J.G. Leong, T.D. Allston, K.J. Reed, A study of lattice expansion in CeO_2 nanoparticles by transmission electron microscopy, J. Phys. Chem. C 113 (2009) 15155–15159.

37. W. Li, S. Man, G. Yang, Y. Mao, J. Luo, L. Cheng, D. Gengzang, X. Xu, S. Yan, Preparation, characterization and gas sensing properties of pure and Ce doped ZnO hollow nanofibers, Mater. Lett. 138 (2015) 188–191.

38. G.X. Wan, S.Y. Ma, X.B. Li, F.M. Li, H.Q. Bian, L.P. Zhang, W.Q. Li, Synthesis and acetone sensing properties of Ce-doped ZnO nanofibers, Mater. Lett. 114 (2015) 103-106.

39. S. Yan, S. Ma, X. Xu, Y. Lu, H. Bian, X. Liang, W. Jin, H. Yang, Synthesis and gas sensing application of porous CeO2–ZnO hollow fibers using cotton as biotemplates, Mater. Lett. 165 (2016) 9-13.

40. T. Li, W. Zeng, Z. Wang, Quasi-one-dimensional metal-oxide-based heterostructural gas-sensing materials: A review, Sens. Actuators B: Chem. 221 (2015) 1570–1585.

41. M. V. Ryzhkov, V. M. Markushev, Ch. M. Briskina, S. I. Rumyantsev, A. P. Tarasov, V. L. Lyaskovskii, Influence of surface plasmon resonance on ZnO films photoluminescence- Role of excitation level, J. Nanoelectron. Optoelectron. 9 (2014) 769-772.

42. R. Kumar, G. Kumar, M.S. Akhtar, A. Umar, Sonophotocatalytic degradation of methyl orange using ZnO nano-aggregates, J. Alloys Compd. 629 (2015) 167-172.

43. Z. Guo, Y. Zhu, F. Meng, F. Du, Facile reflux method synthesis, photo-catalyst and electrochemical properties of micro-sized subuliform CeO_2, Sci. Adv. Mater. 6 (2014) 2688-2693.

44. A. Umar, R. Kumar, G. Kumar, H. Algarni, S.H. Kim, Effect of annealing temperature on the properties and photocatalytic efficiencies of ZnO nanoparticles, J. Alloys Compd. 648 (2015) 46-52.

45. M. Shirzad-Siboni, A. Khataee, B. Vahid, S. W.Joo, Synthesis, characterization and immobilization of ZnO nanosheets on scallop shell for photocatalytic degradation of an insecticide, Sci. Adv. Mater. 7 (2015) 806-814.

46. S.H. Kim, A. Umar, R. Kumar, H. Algarni, G. Kumar, Facile and rapid synthesis of ZnO nanoparticles for photovoltaic device application, J. Nanosci. Nanotechnol. 15(9) (2015) 6807-6812.

47. R. Mohan, G.-S. Kim, S.-J. Kim, ZnO nanostructures in vapor transport growth method, Sci. Adv. Mater. 6 (2014) 336-342.

48. S.R. Balakrishnana, U. Hashima, G.R. Letchumanan, M. Kashif, A.R. Ruslinda, W.W. Liu, P. Veeradasan, R. Haarindra Prasad, K.L. Foo, P. Poopalan, Sens. Actuators, A 220 (2014) 101–111.

49. M. Ding, D. Zhao, B. Yao, X. Xu, ZnO multi-branched microflowers: fabrication and temperature-dependent photoluminescence properties, Sci. Adv. Mater. 6 (2014) 197-201.

50. A. Shrivastava, V.B. Gupta, Methods for the determination of limit of detection and limit of quantitation of the analytical methods, Chron. Young. Sci. 2 (2011) 21-25.

51. M. Abaker, G.N. Dar, A. Umar, S.A. Zaidi, A.A. Ibrahim, S. Baskoutas, A. Al-Hajry, CuO nanocubes based highly-sensitive 4-nitrophenol chemical sensor,Sci. Adv. Mater.4(8) (2012) 893-900

52. S.S. Arbuj, N. Rumale, A. Pokle, J. D. Ambekar, S. B. Rane, U. P. Mulik, D. P. Amalnerkar, Synthesis of photoluminescent ZnO nanopencils and their photocatalytic performance, Sci. Adv. Mater. 6 (2014) 269-275.

53. R. Lamba, A. Umar, S.K. Mehta, S.K. Kansal, Well-crystalline porous ZnO–SnO$_2$ nanosheets: An effective visible-light driven photocatalyst and highly sensitive smart sensor material, Talanta, 131 (2015) 490-498.

54. N. Perinka, M. Držková, D. V. Randjelovic, P. Bondavalli, M. Hajná, P. Bober, T. Syrový, Y. Bonnassieaux, J. Stejskal, Characterization of polyaniline-based ammonia gas sensors prepared by means of spray coating and ink-jet printing, Sensor Lett. 12 (2014) 1620-1627.